

Calculative and experimental study of the CFRP tape spring[†]

Yu-di Zuo^{1,2,*}, Guang Jin¹ and Peng Xie¹

¹Changchun Institute of Optics, Fine Mechanics and Physics, Chinese Academy of Sciences, Changchun 130033, China

²University of Chinese Academy of Sciences, Beijing 100059, China

(Manuscript Received March 30, 2017; Revised March 9, 2018; Accepted April 19, 2018)

Abstract

A tape spring is a thin-walled, straight strip of material with curved cross-section, and the current trend is towards tape springs made of carbon fibre reinforced plastic (CFRP). In this paper, performance of the CFRP tape spring was studied and its bending moment's calculative formula during opposite-sense bending process was derived, also, the theoretical formula's accuracy was assessed by means of detailed, non-linear finite-element analysis. Subsequently, a CFRP tape spring was practical designed and manufactured through twining-moulding workmanship, and some experiments were conducted to study its bending characters, verifying the validity of the theoretical analysis and finite element simulation perfectly.

Keywords: Tape springs; Carbon fibre reinforced plastic (CFRP); Non-linear finite element analysis; Bending moment

1. Introduction

Tape spring becomes more and more arrestive because of its favorable engineering characters in recent years. And deployable structures made of tape springs have low masses, simple mechanics, high efficiency of enfoldment, and have no mechanical joints, also, they can deploy spontaneously without external driving forces [1, 2]. Typical tape springs manufactured by metallic materials such as beryllium-copper or high-strength steel, have been used in space deployable structures for decades, but with the current deployable structures' requirement of cheaper, simpler and more reliable, the carbon fibre reinforced plastic (CFRP) tape springs becomes more and more preponderant, for their tailorable performance, low mass, and low coefficient of thermal expansion [3].

A tape spring can be folded in equal sense and opposite sense, which can both provide driving moment when it has unfolded. The maximum moment in opposite-sense bending is much bigger than that in equal-sense bending. A metallic tape spring's opposite-sense bending behavior has been first studied by Wuest [4]. Later tape springs' large-deflection torsional and flexural behavior was studied by Mansfield [5]. Seffen and Pellegrino then studied the deployment dynamics of a tape spring scrupulously [6]. Also, Soykasap studied the performance of four tape-spring hinges, comprising pairs of short-length metallic elastic tape-spring side by side but

mounted in different ways [7].

Although moment-rotation behavior of a metallic tape spring made of isotropic material has been studied maturely, the behavior of the CFRP tape spring is quite complex because its orthotropic material properties and some negative moments in moment-rotation profile might appear during its bending process and deployment. This paper concentrates on the design of tape springs constructed from a small number of CFRP layers laminated in designed directions and styles having an orthotropic property. Computational formula of the CFRP tape spring's bending moment has been derived based on the theory of thin shell structures, and a practical design was performed, also, the finite element model was established to analysis the designed CFRP tape spring's buckling behavior. Subsequently, the CFRP tape spring was manufactured through twining-moulding method, and some experiments were conducted to study its buckling behavior, verifying the validity of the theoretical analysis and finite element simulation perfectly.

2. Theoretical analysis of the CFRP tape spring

2.1 The material properties of the CFRP tape spring

The CFRP tape spring will generate some biggish deformation along its longitudinal direction as well as some small deformation in its transverse direction during its buckling process, making it mainly subject the longitudinal load as well as some teeny transverse load, moreover, the lay-up direction and style of the CFRP material are generally designed based on its affording loads. The CFRP's 0° lay-up mainly subjects

*Corresponding author. Tel.: +86 43186708025, Fax.: +86 43186708823

E-mail address: zuoyd1809@163.com

[†]Recommended by Editor Chongdu Cho

© KSME & Springer 2018

Table 1. Material properties of the M40JB.

Elastic modulus (GPa)	50
Shear modulus (GPa)	6.2
Poisson's ratio	0.3
Extensional rate (%)	2.0
Density (g/cm ³)	1.78

the axial load, and the $\pm 45^\circ$ lay-up mainly subjects the shear load, while the 90° lay-up mainly subjects the transverse load and regulate the CFRP material's Poisson ratio. Consequently, the CFRP tape spring in this paper adopts the $[0^\circ, 90^\circ]$ lay-up style in order to make it endure the buckling loads more effectively.

The CFRP tape spring in this paper is manufactured through the twining-moulding workmanship by the M40JB carbon plain-weave, which consists of a set of parallel, longitudinal (warp) fibre tows and a set of transverse fibre tows (fill) at 90° that pass alternately under and over the longitudinal tows. This is the most common weave style, and this material has a fiber content up to 68 % percent, making it the most readily available material for tape spring's manufacture due to its symmetrical and balanced properties. The CFRP tape spring made of this material can preferably endure the buckling load, coupling with high strength and low weight, also, its coefficient of thermal expansion and elastic modulus can be regulated by controlling the kind and content of the epoxy resin used in the CFRP, and the CFRP tape spring's manufacturing craft can be well controlled [8, 9], hence, the CFRP material is more appropriate for manufacturing tape spring comparing with other materials.

The material properties related to CFRP tape spring are its elastic modulus E and Poisson ratio μ , and the CFRP tape spring in this paper adopts the $[0^\circ, 90^\circ]$ lay-up style, Table 1 shows some of its material properties, obtained from the experimental tests by the Changchun Aerospace Composite Materials Co., Ltd.

2.2 The geometrical parameters of the tape spring

A CFRP tape spring's major geometrical parameters include its laminates' thickness t , transverse radii of curvature R , angle subtended by cross-section θ , and its length L . All those geometrical parameters will affect the CFRP tape spring's mechanical properties obviously, and it can be folded in equal-sense bending and opposite-sense bending, see Fig. 1 [7].

2.3 Theoretical analysis

The tape spring's buckling behavior of equal-sense bending and opposite-sense bending exist big differences. When a tape spring subjects the external opposite-sense bending moment, it will show higher rigidity at initial stage, then its rigidity will suddenly break down coupling with a sudden snap accompa-

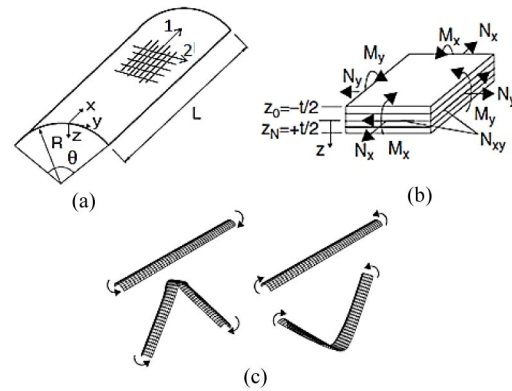


Fig. 1. A CFRP tape spring's geometrical parameters and folding types.

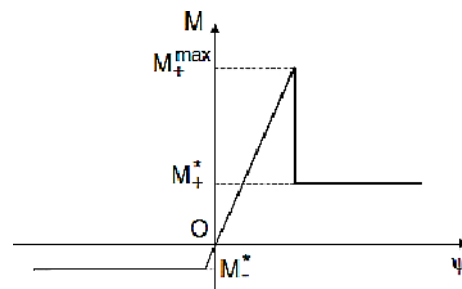


Fig. 2. A tape spring's schematic moment-rotation relationship.

nied by the formation of an elastic fold as the external moment reaches the tape spring's critical moment M_+^{max} , and its bending moment will drop down and gradually stabilize at the tape spring's opposite-sense steady moment M_+^* . Similarly, when a tape spring subjects the external equal-sense bending moment, it will show lower rigidity so that even a small external moment can make it have a big deformation, and its bending moment will finally stabilize at the tape spring's equal-sense steady moment M_-^* , Fig. 2 shows the schematic moment-rotation relationship of a tape spring [10]. The opposite-sense bending character makes tape springs have ideal dynamical property for self-latching components in some precision deployable structures, therefore, this paper commits to study the CFRP tape spring's opposite-sense bending behavior for the future application.

Wuest [3] first obtained a metallic tape spring's moment-curvature relationship during its opposite-sense bending process through experiments and mathematical integration. Wuest considered a tape spring loaded by end moments that impose a uniform longitudinal curvature, and determined the moment-curvature relationship for a slightly distorted axial-symmetric cylindrical shell. But the CFRP tape spring is normally manufactured by a number of fabric plain-weaves which laminated in designed directions, making it have orthotropic material properties. And Wuest's relationship aims at tape springs made of isotropic materials, inappropriate for the CFRP tape springs made of orthotropic material, so the theoretical formulas for CFRP tape springs should be derivated in depth.

According to the theory of thin shell structures [7, 11], a tape spring's bending moments in per unit length for the curvature changes k_x, k_y , on the assumption that $k_{xy} = 0$ are:

$$M_x = D_{11}k_x + D_{12}k_y \quad (1)$$

$$M_y = D_{12}k_x + D_{22}k_y \quad (2)$$

where k_x and k_y is the tape spring's curvature changing in the longitudinal direction and transverse direction respectively. Assuming that the tape spring's curvature changes from zero to $1/r$ in its longitudinal direction, so the deformed configurations of the tape are:

$$k_x = \frac{1}{r} \quad (3)$$

$$k_y = \frac{1}{R} - \frac{d^2 p}{dy^2} \quad (4)$$

where p is the tape spring's out-of-plane deflection in the z -direction. Substituting Eqs. (3) and (4) into Eqs. (1) and (2):

$$M_x = D_{11}\frac{1}{r} + D_{12}\left(\frac{1}{R} - \frac{d^2 p}{dy^2}\right) \quad (5)$$

$$M_y = D_{12}\frac{1}{r} + D_{22}\left(\frac{1}{R} - \frac{d^2 p}{dy^2}\right) \quad (6)$$

According to the differential equation of equilibrium:

$$\frac{d^2 M_y}{dy^2} - \frac{N_x}{r} = 0 \quad (7)$$

$$N_x = \frac{-A_{11}p}{r} \quad (8)$$

where N_x is the normal force per unit length. Substituting Eqs. (7) and (8) into Eq. (6) can obtain a fourth order ordinary differential equation:

$$\frac{d^4 p}{dy^4} + \frac{4f^4 p}{r^4} = 0 \quad (9)$$

where $f = \sqrt[4]{A_{11} / (4D_{22}r^2)}$. The Eq. (9)'s solution of can be obtained as follows:

$$p = b_1 \cosh \frac{fy}{r} \cos \frac{fy}{r} + b_2 \sinh \frac{fy}{r} \sin \frac{fy}{r} \quad (10)$$

where $y = \pm s/2$, $s = 2R \sin(\theta/2)$, and s represents the transverse width of the tape spring. The constants b_1 and b_2 are:

$$b_{1,2} = \mp \frac{r^2}{2f^2} \left(\frac{1}{R} + \mu k_x \right) \frac{\cosh \frac{fs}{2r} \sin \frac{fs}{2r} \mp \sinh \frac{fs}{2r} \cos \frac{fs}{2r}}{\cosh \frac{fs}{2r} \sinh \frac{fs}{2r} + \cos \frac{fs}{2r} \sin \frac{fs}{2r}} \quad (11)$$

where $\mu = D_{12}/D_{22}$, representing the Poisson ratio of the tape spring. Thus, the tape spring's bending moment is then obtained by integrating moments about the y -axis:

$$M = \int_{-s/2}^{s/2} (M_x - N_x p) dy \quad (12)$$

$$= sD_{11} \left(k_x + \frac{\mu}{R} - \mu \left(\frac{1}{R} \mu k_x \right) F_1 + \frac{1}{k_x} \left(\frac{1}{R} + \mu k_x \right)^2 F_2 \right)$$

where y and M_x represents the tape spring's length and bending moment per unit length, respectively. F_1 and F_2 can be obtained by the Eq. (13):

$$F_1 = \frac{2 \cosh \lambda - \cos \lambda}{\lambda \sinh \lambda + \sin \lambda}, \quad F_2 = \frac{F_1}{4} - \frac{\sinh \lambda \sin \lambda}{(\sinh \lambda + \sin \lambda)^2} \quad (13)$$

where $\lambda = fs/r = \sqrt[4]{3(1-\mu^2)}s/\sqrt{t/k_x}$. M_+^{max} , the tape spring's critical buckling moment, is the maximum moment obtained by maximizing with respect to r , representing a tape spring's supporting stiffness when deployed and self-latched. The bigger the value of M_+^{max} , the better anti-jamming performance and stiffness of a tape spring.

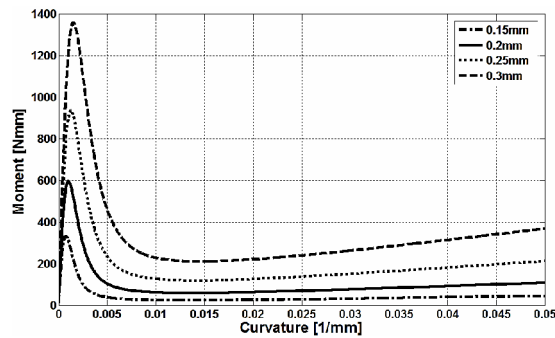
Eq. (12) is the bending moment computational formula of a CFRP tape spring in opposite-sense bending, which reflects its bending moment changing trends in the whole buckling and bending process. A CFRP tape spring's buckling behavior is mainly depended on its material properties and geometrical parameters according to the Eq. (12). Note that $E_1 = E_2$, as the CFRP tape spring's in this paper laying-up in orthotropic laminates, so it follows that all laminates have equal extensional stiffness and bending stiffness, also, those material properties of the CFRP tape spring can be seen in Table 1. Moreover, the CFRP tape spring's pivotal geometrical parameters are its laminates' thickness t and angle subtended by cross-section θ . Next, single-variable analytical method has been conducted in order to study the influencing and sensitive extent of this two parameters to the CFRP tape spring expediently.

Maintaining the CFRP tape spring's transverse radii of curvature $R = 20$ mm and its $[0^\circ, 90^\circ]$ lay-up style, when its subtended angle $\theta = 90^\circ$, its moment-curvature relationship under different thicknesses t can be seen in Fig. 3(a). As the same, when the CFRP tape spring's thickness $t = 0.2$ mm, its moment-curvature relationship under different subtended angles θ can be seen in Fig. 3(b).

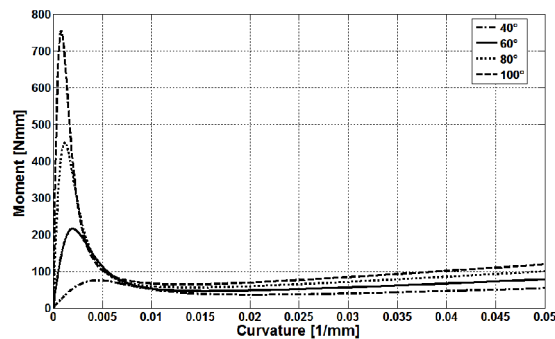
Some conclusions can be obtained according to the Fig. 3: (1) When the CFRP tape spring's subtended angle θ (or laminates' thickness t) is maintained as a constant, its critical bending moment M_+^{max} will increase obviously with the increment of t (or θ) respectively, and its opposite-sense steady moment M_+^* will modestly increase either. Also, the geometrical parameter of laminates' thickness t affects the CFRP tape spring's bending moment more distinctly. (2) With increment

Table 2. Geometric parameters of the designed CFRP tape spring.

Length, L	180 mm
Transverse radii of curvature, R	20 mm
Subtended angle, θ	90°
Thickness, t	0.3 mm
Lay-up style	$[0^\circ, 90^\circ]_2$



(a) Moment-curvature graph under different thicknesses



(b) Moment-curvature graph under different subtended angles

Fig. 3. CFRP tape spring's moment-curvature relationships.

of the CFRP tape spring's bending curvature k_x in its longitudinal direction, its bending moment will increase rapidly at the initial stage and gradually drop down stabilizing at its opposite-sense steady moment M_+^* .

In order to verify the validity of the theoretical analysis above, a practical design of the CFRP tape spring will be conducted next combined with the need of a deployable structure attributed to an engineering project, also, the finite element simulation and experiments will be carried out to study the designed CFRP tape spring's buckling behavior. Where the deployable structure requires the CFRP tape spring satisfy some indexes as follows: The CFRP tape spring should be 180 mm in length and its critical moment should exceed than 1000 Nmm coupling with that it can be folded 180° in opposite-sense direction repeatedly. The practical designed CFRP tape spring's geometrical parameters can be determined according to the above theoretical analysis, see Table 2.

The designed CFRP tape spring's moment-curvature relationship can be obtained by Eq. (12) through the MATLAB [12] software, and its critical bending moment M_+^{max} is 1356 Nmm, making it have a relatively high stiffness, see Fig.

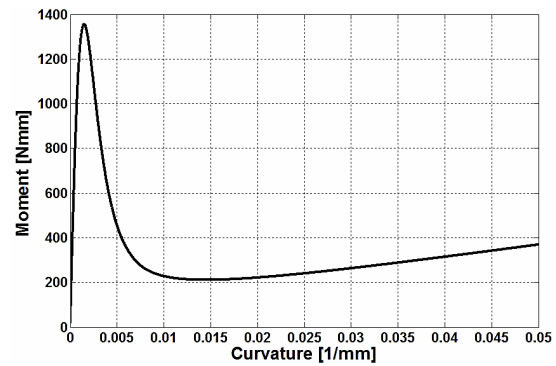


Fig. 4. Moment-curvature relationship of the CFRP tape spring.

4. Moreover, the designed CFRP tape spring will show higher rigidity and remain self-latching state before the external opposite-sense bending moment reaches its M_+^{max} , and its stiffness will reduce sharply coupling with a sudden snap accompanied by the formation of an elastic fold when the external moment exceeds its critical bending moment. These opposite-sense bending characteristics make the CFRP tape spring have ideal dynamical properties for self-latching components in some precision deployable structures.

3. Finite element simulations

The CFRP tape spring has been preliminary designed after determining its orthotropic material properties and geometrical parameters through the theoretical analysis above. Subsequently, the ABAQUS [13] software was used to establish the CFRP tape spring's finite element model (FEM) and simulate its opposite-sense buckling behavior. The whole CFRP tape spring's element model used the thin shell elements which were 4-node reduced integration shell elements (S4R5), performing properly for large rotations with only small strains. Moreover, MPC, which means multi-point constraints mainly used to control the degree of freedom between nodes, were used to define the boundary conditions, and the nodes on either end of the CFRP tape spring were tied to a MPC node, located at the centroid of the tape spring's end cross section which can ensure it subject pure bending moment, using the RBE2 rigid elements, which usually used to simulate the rigid connection of two parts. When the CFRP tape spring's material properties, geometrical parameters and lay-up style have been defined to its established FEM, a geometrically non-linear incremental analysis was carried out using the Newton-Raphson solution method, and Fig. 5 shows the CFRP tape spring's finite element model.

The CFRP tape spring is subjected to opposite-sense bending under monotonically increasing end rotations of the two MPC nodes. Fig. 6 shows the moment-rotation relationship of a $[0^\circ, 90^\circ]_2$ M40JB tape spring with $R = 20$ mm, $\theta = 90^\circ$ and $t = 0.3$ mm. The CFRP tape spring's critical bending moment attains 1276.5 Nmm when its rotation reaches to 7.9°, while, Fig. 6 shows that the tape spring's critical bending moment is 1356 Nmm when its longitudinal bending curvature reaches to

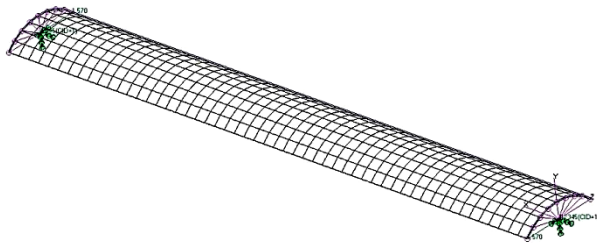


Fig. 5. Finite element model of the CFRP tape spring.

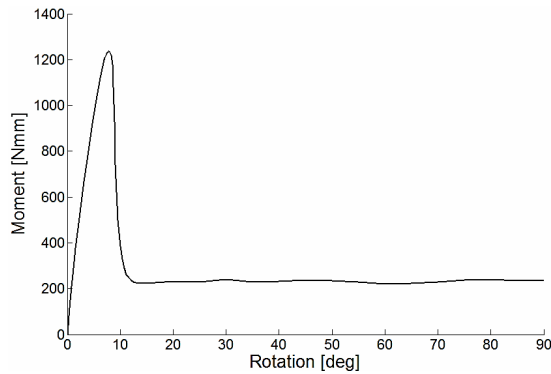


Fig. 6. CFRP tape spring's moment-rotation relationship through FEA.

0.002 mm^{-1} . Comparing the curve in Fig. 4 with Fig. 6 can obtain that the changing trends of the designed CFRP tape spring's bending moment are approximately accordant. Furthermore, the CFRP tape spring's critical bending moment under finite element simulation and theoretical analysis are approximately equivalent, and the relative error between them is about 5.9 %.

4. Experimental study of the CFRP tape spring

4.1 Measurement of the CFRP tape spring's bending moments

In order to verify the theoretical analysis and finite element simulation above more accurately, the practically designed CFRP tape spring is manufactured through the twining-moulding method by using the M40JB carbon plain-weave compounding some epoxy resins, and experiments have been conducted to study its buckling behavior. The manufactured CFRP tape spring has two-ply laminates and adopts the $[0, 90^\circ]$ lay-up style, see Fig. 7.

Subsequently, tests of the manufactured CFRP tape spring's moment-rotation relationship were carried out using the laboratorial bending apparatus, and measurements of the tape spring's curvature-rotation relationship were conducted using the projective mapping method, see Fig. 8. The tested data of the bending apparatus were noted during the experiment to import in the MATLAB software, obtaining the CFRP tape spring's moment-rotation relationship during its opposite-sense bending as shown in Fig. 9(a). As the same, the multiple test data of the CFRP tape spring's rotations through projective mapping method were noted and its relevant curvatures in

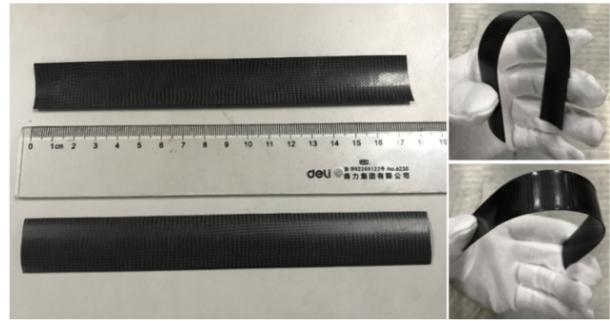


Fig. 7. The manufactured CFRP tape spring.

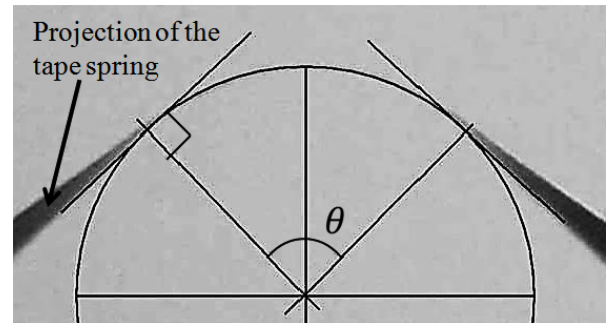


Fig. 8. Measurement of the bend curvature and rotation.

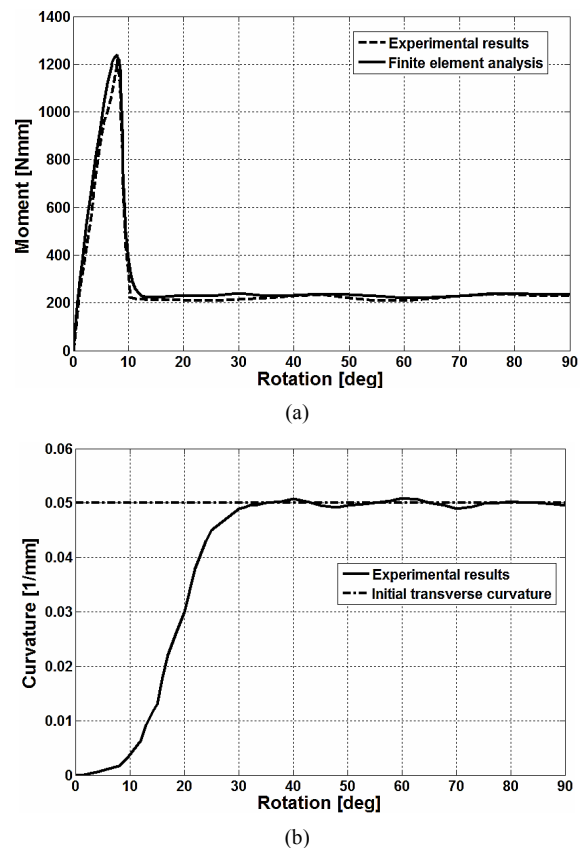


Fig. 9. (a) The CFRP tape spring's moment-rotation relationship; (b) the CFRP tape spring's curvature-rotation relationship.

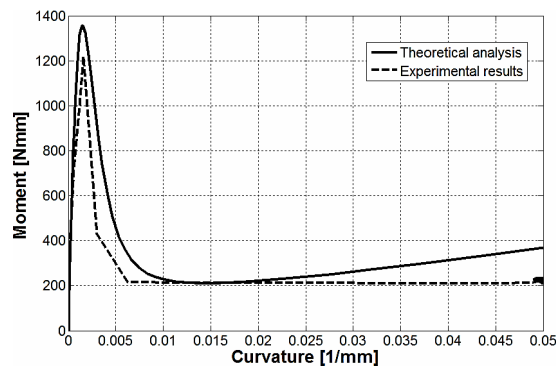


Fig. 10. The CFRP tape spring's moment-curvature relationship.

longitudinal direction were calculated and averaged, next, all these data were imported in the MATLAB software, obtaining the CFRP tape spring's curvature-rotation relationship during its opposite-sense bending as shown in Fig. 9(b).

Some conclusions can be obtained from Fig. 9: (1) The manufactured CFRP tape spring's moment-rotation relationship through experimental tests is quite coincident with its finite element analysis (FEA) results, and the CFRP tape spring's critical bending moment attains 1237.6 Nmm when its rotation reaches to 8° , agreeing with its theoretical analysis result and FEA result properly. (2) The CFRP tape spring's curvature in its longitudinal direction changes slightly at initial stage, but then changes greatly when its rotation reaches about 8° and finally stabilizes at the curvature of its initial cross-section circle $1/R = 0.05 \text{ mm}^{-1}$.

Combining the curvature-rotation curve in Fig. 9(b) with the moment-rotation curve in Fig. 9(a) can obtain the CFRP tape spring's moment-curvature relationship through experiments, see Fig. 10. The CFRP tape spring's moment-curvature relationship through experiments and theoretical analysis are accordant properly, and experimental results show that the tape spring's critical moment attains 1237.6 Nmm when its curvature reaches about 0.002 mm^{-1} , matching the experimental and FEA results well with a maximum relative error of 8.7 %. Consequently, the validity of previous theoretical analysis and finite element simulation has been verified further more through the experiments above.

4.2 Error analysis

The maximum relative error of the manufactured CFRP tape spring's critical bending moment between theoretical analysis, finite element simulation and experiment is 8.7 % from the study above, so it is necessary to analysis the causes of this error.

(1) The main errors during the finite element simulation are: the FEA's computational program is approximately realized by discretizing continuous objects, so the finite elements' quantity and computational program will affect the FEA's solving accuracy distinctly. The imprecise boundary constraints, external loads and material's properties introduced to

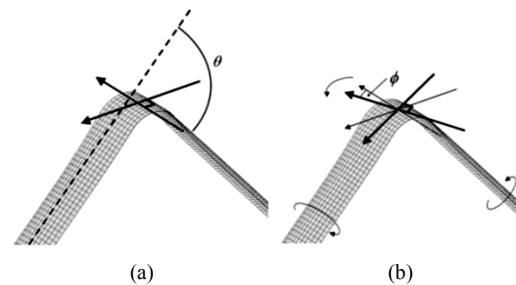


Fig. 11. The CFRP tape spring's bending behavior: (a) Buckling behavior during theoretical analysis and FEA; (b) buckling behavior during experiments.

the FEM will also affect the FEA's solving accuracy.

(2) The main errors during experiments are the measuring equipments and factitious manipulations' errors. The CFRP tape spring generated a major bending deformation as well as some slight torsional distortion along its longitudinal direction [10] (see Fig. 11(b)) during experiments, making the experimental test results weren't the CFRP tape spring's pure bending moment. While the theoretical analysis and FEA results were obtained under the assumption that the tape spring couldn't generate torsional distortions along its longitudinal direction (see Fig. 11(a)), making the experimental test moment smaller than the pure bending moment obtained by theoretical analysis and FEA, and causes the errors in depth. The manipulator's numerical reading, projective drawing, and approximately calculative errors during measuring the CFRP tape spring's curvatures and rotations also would cause some inevitable errors.

5. Conclusion

This paper has systematically studied the CFRP tape springs' bulking behaviors through theoretical analysis, finite element simulation and experimental tests, drawing some conclusions as follows:

(1) The CFRP tape springs made from a few plies of woven carbon fibre laminated in designed directions have an orthotropic material property, and controlling the epoxy's content reasonably can make the CFRP tape springs have better deployable characters and more suitable for constructing some deployable structures;

(2) The CFRP tape spring's opposite-sense bending moment, and its sensitive parameters, critical bending moment as well as its bending moment changing trends during its opposite-sense bending process can be obtained from the calculative formula (Eq. (12)), which can guide the design of CFRP tape springs;

(3) The non-linear finite element analysis method has been provided for analyzing the CFRP tape spring's buckling behavior. The CFRP tape spring manufactured through the twin-molding method has better bulking behaviors, and experiments have been conducted to study its buckling behaviors. Experiments confirmed the accuracy of theoretical analysis

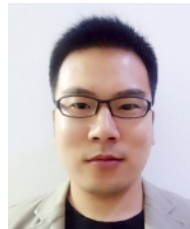
and finite element simulation well. Consequently, theoretical and technical supports could be provided for the future design and applications of CFRP tape springs.

Acknowledgments

This work has been supported by National High Technology Research and Development Program of China (The 863 Program), No. 2015AA7015090.

References

- [1] K. A. Seffen, Z. You and S. Pellegrino, Folding and deployment of curved tape springs, *International Journal of Mechanical Science*, 42 (10) (2000) 2055-2073.
- [2] K.-W. Kim and Y. Park, Solar array deployment analysis considering path-dependent behavior of a tape spring hinge, *Journal of Mechanical Science and Technology*, 29 (5) (2015) 1921-1929.
- [3] M. Eigenmann et al., Ultra-light deployment mechanism (UDM) for sectioned large deployable antenna reflectors, *Proc. 14th European Space Mechanisms & Tribology Symposium-ESMATS* (2011) 479-481.
- [4] W. Wuest, Einigenwendungen der theorie der zylinder-schale, *Zeitschrift für Angewandte Mathematik und Mechanik*, 34 (12) (1954) 444-454.
- [5] E. H. Mansfield, Large-deflection torsion and flexure of initially curved strips, *Proceedings of the Royal Society London (A334)* (1973) 279-298.
- [6] K. A. Seffen and S. Pellegrino, Deployment dynamics of tape springs, *Proceedings of the Royal Society of London A: Mathematical, Physical and Engineering Sciences*, 455 (1983) (1999) 1003-1048.
- [7] O. Soykasap, Analysis of tape spring hinges, *International Journal of Mechanical Sciences*, 49 (7) (2007) 853-860.
- [8] K.-H. Im, I.-Y. Yang, S.-K. Kim, J.-A. Jung, Y.-T. Cho and Y.-D. Woo, Terahertz scanning techniques for paint thickness on CFRP composite solid laminates, *Journal of Mechanical Science and Technology*, 30 (10) (2016) 4413--4416.
- [9] O. A. Abdullah and A. K. F. Hassan, Effect of prestress level on the strength of CFRP composite laminate, *Journal of Mechanical Science and Technology*, 30 (11) (2016) 5115-5123.
- [10] S. J. I. Walker and G. S. Aglietti, A study of tape spring fold curvature for space deployable structures, *Proceedings of the Institution of Mechanical Engineers, Part G: Journal of Aerospace Engineering*, 221 (3) (2007) 313-325.
- [11] Z. Wong and Y. Wang, *Elastic theory on thin shell*, Higher Education Press, Beijing, China (1986).
- [12] G. J. Borse, *Numerical method with MATLAB: A resource for scientists and engineers*, International Thomson Publishing, London, Britain (1997).
- [13] ABAQUS, Inc, *ABAQUS theory and standard user's manual*, Version 6.4, Pawtucket, USA (2003).



Yu-di Zuo (1990-) graduated in the JinLin University of China, and as a Ph.D. in Changchun Institute of Optics, Fine Mechanics and Physics. He mainly concentrates on the design of space deployable structures, and non-linear finite element analysis, corresponding. E-mail: zuoyd1809@163.com.